THE JOURNAL OF BIOLOGICAL CHEMISTRY VOL. 286, NO. 19, pp. 16768–16774, May 13, 2011

Glucagon-like Peptide 1 Stimulates Post-translational Activation of Glucokinase in Pancreatic β Cells*[S]

Received for publication, October 11, 2010, and in revised form, March 21, 2011 Published, JBC Papers in Press, March 25, 2011, DOI 10.1074/jbc.M110.192799

Shi-Ying Ding, Andongfac Nkobena, Catherine A. Kraft, Michele L. Markwardt, and Mark A. Rizzo[1]

From the Department of Physiology, University of Maryland School of Medicine, Baltimore, Maryland 21201

Glucagon-like peptide 1 (GLP-1) potentiates glucose-stimulated insulin secretion from pancreatic β cells, yet does not directly stimulate secretion. The mechanisms underlying this phenomenon are incompletely understood. Here, we report that GLP-1 augments glucose-dependent rises in NAD(P)H autofluorescence in both βTC3 insulinoma cells and islets in a manner consistent with post-translational activation of glucokinase (GCK). GLP-1 treatment increased GCK activity and enhanced GCK *S*-nitrosylation in βTC3 cells. A 2-fold increase in *S*-nitrosylated GCK was also observed in mouse islets. Furthermore, GLP-1 activated a FRET-based GCK reporter in living cells. Activation of this reporter was sensitive to inhibition of nitric-oxide synthase (NOS), and incorporating the *S*-nitrosylation-blocking V367M mutation into this sensor prevented activation by GLP-1. GLP-1 potentiation of the glucose-dependent increase in islet NAD(P)H autofluorescence was also sensitive to a NOS inhibitor, whereas NOS inhibition did not affect the response to glucose alone. Expression of the GCK(V367M) mutant also blocked GLP-1 potentiation of the NAD(P)H response to glucose in βTC3 cells, but did not significantly affect metabolism of glucose in the absence of GLP-1. Co-expression of WT or mutant GCK proteins with a sensor for insulin secretory granule fusion also revealed that blockade of post-translational GCK *S*-nitrosylation diminished the effects of GLP-1 on granule exocytosis by ~40% in βTC3 cells. These results suggest that post-translational activation of GCK is an important mechanism for mediating the insulinotropic effects of GLP-1.

Glucagon-like peptide 1 (GLP-1)[2] can potentiate glucose-stimulated insulin secretion at glucose concentrations that are normally subthreshold, in the 3–5 mM range, but not at glucose concentrations less than that (1–3). In pancreatic β cells, the glucose threshold for insulin secretion is strongly controlled by glucose metabolism and principally limited at the first metabolic step, which is conversion of glucose to glucose 6-phosphate (4). Glucokinase (GCK) activity largely controls the rate of secretion at this step in metabolism because of its weak glucose binding affinity. Half-maximal GCK activity occurs at ~8 mM (4, 5), and sufficient glucose metabolism to initiate secretion is observed at ~5 mM (6, 7). Therefore, changes in GCK activity are a likely control point for changes in threshold.

Secretion at glucose levels that are normally subthreshold is possible if glucose-phosphorylating capacity is artificially modulated through overexpression of exogenous hexokinases (8) or GCK itself (9). Mathematical modeling of the effect of naturally occurring GCK mutations on secretion has also shown a tight relationship between GCK activity and the threshold for insulin secretion (10). Furthermore, mutations that enhance GCK activity reduce the glucose threshold for insulin secretion (11). Thus, there are similarities between the effects of enhancing GCK activity and the effects of incretin hormones on insulin secretion.

Glucose metabolism may also be acutely regulated through post-translational activation of GCK. In an unstimulated state, GCK binds to secretory granules (12, 13) through association with nitric-oxide synthase (NOS) (14). Dissociation of this complex, either through receptor activation or disruption of NOS dimerization (15), stimulates GCK translocation to the cytoplasm (16). Activation is generally mediated through post-translational *S*-nitrosylation of a specific cysteine residue on GCK (14). Diabetes-associated mutations in GCK also have been shown to affect post-translational regulation negatively in the absence of a direct effect on GCK activity *in vitro* (17), indicating that GCK *S*-nitrosylation may be a physiologically important control point for regulating glucose-stimulated insulin secretion. Therefore, regulation of GCK by GLP-1 is an attractive hypothesis not only because this mechanism may explain the insulinotropic effects of GLP-1 at normally subthreshold glucose concentrations, but also because it could provide additional insight into the mechanism through which naturally occurring gene mutations in GCK cause diabetes.

Here, we tested the hypothesis that GLP-1 can post-translationally regulate GCK in mouse pancreatic β cells, and we have found that GLP-1 potentiates the glucose-stimulated increase in NAD(P)H autofluorescence in both βTC3 insulinoma cells and islets. Furthermore, GLP-1 stimulates GCK *S*-nitrosylation, GCK activity, and activation of a FRET-based GCK sensor in living cells. Incorporation of mutation that blocks *S*-nitrosylation into the sensor prevented GLP-1 activation. Furthermore, expression of this mutant GCK in βTC3 cells blocked GLP-1 potentiation of glucose-stimulated changes in NAD(P)H autofluorescence. In islets, pharmacological

* This work was supported, in whole or in part, by National Institutes of Health Grants R21-DK067415, R01-DK077140, and DK077140-02S1 (to M. A. R.) and P60-DK079637 and P30-DK072488.

[S] The on-line version of this article (available at http://www.jbc.org) contains supplemental Figs. S1 and S2.

[1] To whom correspondence should be addressed: 660 W. Redwood St., HH 525B, Baltimore, MD 21201. Tel.: 410-706-2421; Fax: 410-706-8341; E-mail: mrizz001@umaryland.edu.

[2] The abbreviations used are: GLP-1, glucagon-like peptide 1; GCK, glucokinase; L-NAME, N^G-nitro-L-arginine methylester; SEP, superecliptic pHluorin-; SNAP, *S*-nitroso-*N*-acetylpenicillamine; SNO, *S*-nitrosocysteine; TIRFM, total internal reflection fluorescence microscopy; VAMP2, vesicle-associated membrane protein 2.

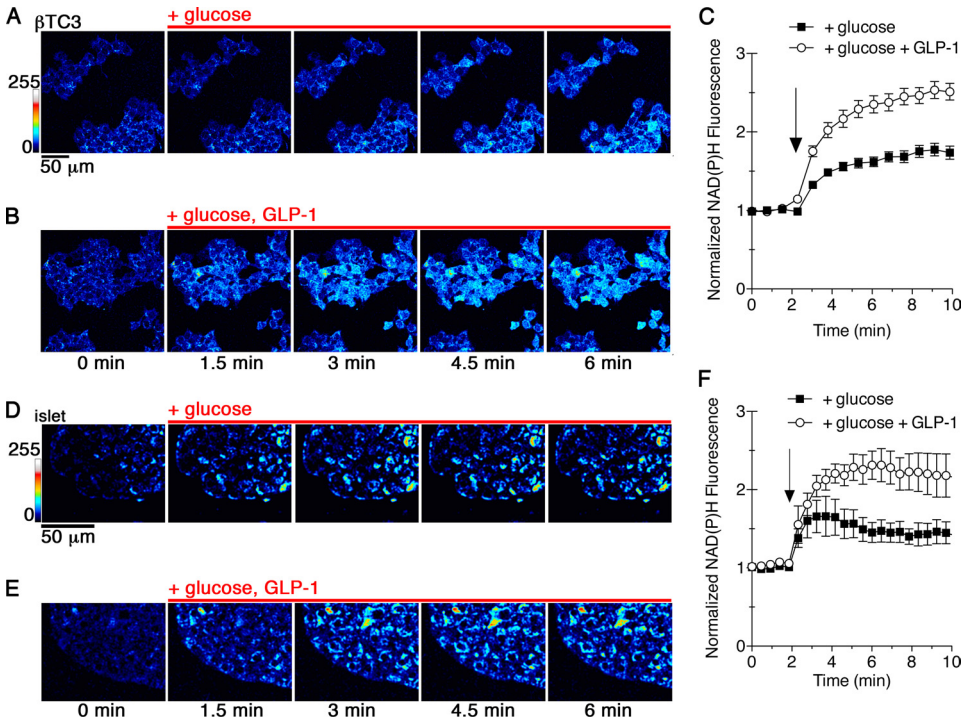

FIGURE 1. **GLP-1 potentiates glucose metabolism in pancreatic β cells.** *A–C*, NAD(P)H autofluorescence from βTC3 cells was captured by two-photon excitation fluorescence microscopy. Glucose-starved cells were stimulated with 5 mM glucose alone (*A*) or in combination with 30 nM GLP-1 (*B*). A pseudocolor lookup table was applied to the images to indicate fluorescence intensity. *C*, time-resolved changes to NAD(P)H were normalized to the mean prestimulated fluorescence for cells treated with glucose (*black squares*) or glucose and GLP-1 (*open circles*). *Points* represent the mean ± S.E. (*error bars*) for $n = 50$ cells. The *arrow* indicates addition of reagents. *D–F*, two-photon images of an islet cultured in 2 mM glucose prior to addition of 5 mM glucose (*D*) or glucose and 30 nM GLP-1 are shown. *E*, changes in NAD(P)H were quantified. The data indicate the average cell responses (±S.E.) from at least 20 cells per islet, $n = 3$ islets. NAD(P)H intensity was normalized to baseline, prestimulation fluorescence. The *a*rrow indicates addition of stimulatory reagents.

inhibition of NOS blocked GLP-1 potentiation of glucose-stimulated rises in NAD(P)H fluorescence, but did not have an effect on islets treated with only glucose. Using a fluorescence marker for insulin secretory granule exocytosis, we also found that GCK activation can account for ~40% of GLP-1 potentiation of exocytosis. Taken together, these data suggest a novel mechanism through which incretin hormones can directly control glucose metabolism in pancreatic β cells.

EXPERIMENTAL PROCEDURES

Reagents—Experiments utilized human GLP-1,7–37 or porcine insulin from Sigma-Aldrich, where indicated. *S*-Nitroso-*N*-acetylpenicillamine (SNAP) was from Invitrogen. Tissue culture media and sera were also obtained from Invitrogen, with the exception of DMEM (Mediatech). Plasmid DNA encoding GCK reporter constructs are described elsewhere (17). Anti-fluorescent protein and anti-nitrosocysteine (SNO) antibodies were from Abcam (Cambridge, MA), and GCK antibodies were obtained from Santa Cruz Biotechnology (Santa Cruz, CA). Horseradish peroxidase-conjugated secondary antibodies were from Jackson Immunoresearch (West Grove, PA). Agarose-conjugated secondary antibodies were from Rockland Immunochemicals (Gilbertsville, PA). All other chemicals were obtained from Sigma-Aldrich, unless otherwise indicated.

Cell Culture—βTC3 cells were cultured as described previously (16). Prior to experimentation, cells were washed in the experimental buffer containing 125 mM NaCl, 5.7 mM KCl, 2.5 mM $CaCl_2$, 1.2 mM $MgCl_2$, 0.1% BSA, and 10 mM HEPES, pH 7.4 (16). Transfections used plasmid DNA purified with kits from Qiagen (Gaithersburg, MD) and FuGENE 6 (Roche Applied Science). Formulations were prepared according to the manufacturer's suggested protocol. Islets were isolated from 6- to 12-week-old male C57/BL6 mice and cultured on human extracellular matrix for microscopy experiments as described previously (18).

Fluorescence Imaging—Fluorescence imaging of NAD(P)H and the FRET-GCK reporters (mCerulean-GCK-mVenus) were performed using a LSM510/META microscope (Carl Zeiss Microimaging, LLC, Thornwood, NY) equipped for two-photon and confocal microscopy as described (17). Quantification was performed with Zeiss AIM software. Data were analyzed using the statistical packages in GraphPad Prism 5 software. Total-internal reflection microscopy (TIRFM) was performed on an AxioObserver fluorescence microscope (Zeiss). 488-nm diode laser illumination was delivered using the TIRF3 slider and the 38 HE GFP filter set. A 1.46 NA/100× Plan-apochromat lens was used to create internal reflection, with the angle of reflection controlled using Zeiss Axiovision software. Collection was with a water-cooled C10600 Orca R2 camera (Hamamatsu, Bridgewater, NJ). Experiments were performed at 37 °C using a Zeiss microscope incubation system. Images were analyzed using ImageJ software (National Institutes of Health). Figure graphics were prepared using Prism software, ImageJ, and Adobe Photoshop.

Biochemical Assays—GCK activity from cell lysates was quantified as described (16). *S*-Nitrosylated proteins were iden-

tified using the biotin-switch assay (19) on untransfected or transfected βTC3 cells, also as described previously (14). For detection of *S*-nitrosylated proteins in pancreatic islets, ~100 islets were incubated in 2.5 mM glucose conditions for 3 h prior to experimentation. Following stimulation, culture medium was carefully aspirated and replaced with 500 μl of lysis buffer (50 mM Tris, pH 7.5, 150 mM NaCl, 2 mM EDTA, 0.1% Triton X-100). Islets were mechanically lysed by passage through a 25.5-gauge needle and incubated for 30 min under constant agitation at 4 °C. GCK proteins were immunoprecipitated using rabbit antibodies and agarose-conjugated secondary antibodies. Immunoprecipitates were analyzed by nonreducing Western blotting, using anti-GCK or anti-*S*-nitrosocysteine antibodies together with Pierce's Fast Western blotting kit. Blot images were captured using a Bio-Rad ChemiDoc XRS and quantified using ImageJ.

Insulin ELISA—βTC3 cells were plated in 6-well dishes and starved in glucose-free Krebs-Ringer buffer (125 mM NaCl, 5.9 mM KCl, 1.28 mM $CaCl_2$, 1.2 mM $MgCl_2$, 25 mM HEPES, pH 7.4, 0.1% BSA) for 4 h prior to experimentation. Cells were incubated with buffer containing 0 or 8 mM glucose with or without 30 nM GLP-1 for 30 min. Insulin secreted into the solution was measured using a rat/mouse insulin ELISA (Millipore), according to the manufacturer's instructions. Insulin secretion was normalized to protein concentrations of cell lysates obtained using the bicinchoninic acid assay kit (Pierce). Values from the glucose-free condition were subtracted from glucose-treated and co-stimulated cells prior to normalization.

Apoptosis Assay—βTC3 cells were plated on No. 1.5 coverslips and incubated in either complete medium, the glucose-free experimental buffer, or with the glucose-free buffer supplemented with 1 μM staurosporine to induce apoptosis. Apoptotic cells were labeled with biotin-X annexin V and streptavidin-conjugated Alexa Fluor® 350 using the Vybrant® Apoptosis Assay kit No. 6 (Invitrogen) according to the manufacturer's instructions. Cells were then fixed in a 4% paraformaldehyde (Electron Microscopy Sciences) solution containing 4% sucrose in PBS, and coverslips were mounted in Prolong® Gold Antifade Reagent (Invitrogen). Observation was with a 20×, 0.75 NA Plan-apochromat objective lens (Zeiss) using a DAPI filter set (No. 49, Zeiss) or transmitted light Nomarski differential interference contrast microscopy. Images were collected using the Orca R2 CCD.

RESULTS

GLP-1 Potentiates the Glucose-stimulated Increase in NAD(P)H Autofluorescence in Pancreatic β Cells—To test whether GLP-1 treatment positively regulates glucose phosphorylation in pancreatic β cells, we examined the glucose-stimulated increase in NADH and NADPH autofluorescence in βTC3 insulinoma cells by two-photon fluorescence microscopy (Fig. 1,*A–C*). Glucose metabolism results in conversion of endogenous, nonfluorescent NAD^+ and $NADP^+$ to fluorescent NADH and NADPH, which are indistinguishable to the detector and are collectively referred to as NAD(P)H (17, 20, 21). Addition of 5 mM glucose to fasting βTC3 cells produced a 50% increase in the endogenous fluorescence over a 5-min period (Fig. 1*C*). Co-stimulation with GLP-1 increased NAD(P)H fluorescence 2-fold over the same period of time compared with treatment with only glucose. Furthermore, fasting of βTC3 cells in glucose-free conditions for a 4-h period did not induce apoptosis or cause morphological changes (supplemental Fig. S1), indicating that the fast was well tolerated. Similar effects on NAD(P)H fluorescence were also observed in pancreatic islets (Fig. 1, *D–F*), with GLP-1 potentiating the glucose response by ~2-fold. GLP-1 can therefore acutely potentiate glucose metabolism in β cells and in islets.

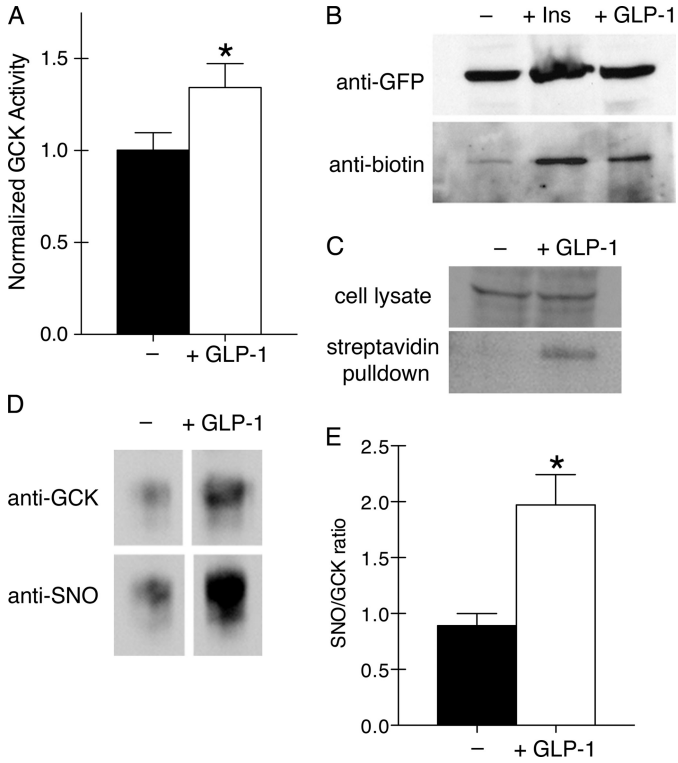

FIGURE 2. **GLP-1 stimulates GCK activation and post-translational *S*-nitrosylation.** *A*, GCK activity was measured from lysates of βTC3 cells that were glucose- and serum-starved (*black*) or treated with 30 nM GLP-1 for 5 min (*white*). *Bars* indicate mean ± S.E. (*error bars*) for $n = 5$ experiments. * indicates significance ($p < 0.05$) as determined by a two-tailed *t* test. *B*, *S*-nitrosylation of GCK-mVenus was observed in transfected cells left untreated (−) or stimulated with either insulin (100 nM, 5 min) or GLP-1 (30 nM, 5 min). *S*-Nitrosylated cysteines were modified with biotin in lysed cells using the biotin-switch assay (14, 19) prior to immunoprecipitation with anti-fluorescent protein antibodies. Precipitates were then Western blotted for the fluorescent protein tag (*top*) or the *S*-nitrosylation-indicating biotin. C, *S*-nitrosylation of endogenous GCK was detected by performing the biotin-switch assay on cell lysates from untreated (−) and GLP-1-treated cells (30 nM, 5 min). Biotinylated proteins were isolated using streptavidin-conjugated agarose beads. GCK was detected by Western blotting on cell lysates and streptavidin pulldowns using anti-GCK antibodies. *D*, islets were treated with 30 nM GLP-1 for 10 min prior to lysis. GCK was immunoprecipitated and assessed for GCK and SNO by Western blotting. *E*, ratio of SNO to GCK was quantified using ImageJ. *Bars* indicate mean ± S.E. (*error bars*) for $n = 4$ experiments. * indicates significance ($p < 0.05$) as determined by a two-tailed *t* test.

Post-translational Activation of GCK—The magnitude of the increase in glucose-stimulated NAD(P)H fluorescence observed with GLP-1 treatment is similar to that associated with post-translational activation of GCK by *S*-nitrosylation (17). To test whether GLP-1 can similarly regulate GCK, we measured GCK activity in GLP-1-treated cells and those left untreated (Fig. 2*A*). GCK activity was significantly stimulated in the GLP-1-treated group (*t* test, $p < 0.05$, $n = 5$). Under these conditions, *S*-nitrosylated GCK was also detected in cells trans-

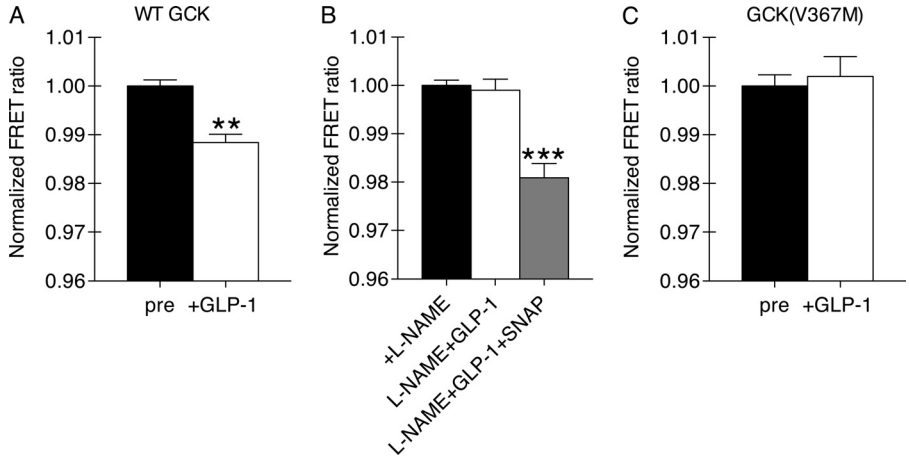

FIGURE 3. **GLP-1 stimulates activation of a FRET-based GCK reporter in living cells.** *A*, βTC3 cells expressing the WT FRET-GCK reporter were stimulated with 30 nM GLP-1 (5 min). The normalized FRET ratio was calculated before (*black*) and after (*white*) stimulation for individual cells. Statistical significance from pretreatment FRET ratio ($p < 0.01$, $n = 7$ cells, two-tailed *t* test) is denoted by **. *B*, cells expressing the WT FRET-GCK reporter were pretreated with the NOS inhibitor L-NAME (5 mM, 10 min) prior to stimulation with GLP-1 (30 nM, 5 min). The same cells were subsequently treated with a NO donor (100 μM, SNAP, 1 min). (***, $p < 0.001$ *versus* L-NAME and prestimulation, ANOVA, Tukey multiple comparison, $n = 7$ cells). *C*, cells expressing a FRET-GCK sensor containing the V367M mutation were treated as in *A*. The poststimulation FRET ratio was not significantly different from the prestimulation FRET ratio ($p > 0.05$, two-tailed *t* test, $n = 8$ cells). *Bars* indicate mean ± S.E. (*error bars*) for all groups.

fected with exogenous GCK fused to a YFP variant (Fig. 2*B*). *S*-Nitrosylation of endogenous GCK was also detected in untransfected cells (Fig. 2*C*). The potency of GLP-1 for stimulating GCK *S*-nitrosylation approximated that of insulin (Fig. 2*B*), and the magnitude of GCK activation was similar to previous results obtained with insulin (16). We were also able to detect *S*-nitrosylated GCK in islets incubated in low glucose- and GLP-1-treated islets by immunoprecipitating with anti-GCK antibodies and Western blotting with an anti-SNO antibody (Fig. 2*C*). GLP-1 stimulated a 2-fold increase in *S*-nitrosylated GCK when normalized to GCK found in the immunoprecipitates (Fig. 2*D*). This observation is consistent with our finding that GLP-1 potentiates glucose metabolism in islets.

Regulation of GCK activation was next tested using a FRET-based GCK biosensor expressed in living βTC3 cells. Activation of the reporter by *S*-nitrosylation produces decreased FRET (14, 17). GLP-1 treatment of glucose-starved βTC3 cells produced sensor activation (Fig. 3*A*). Furthermore, activation of the FRET-based sensor was inhibited by treatment with N^G-nitro-L-arginine methylester (L-NAME), an inhibitor of NOS (Fig. 3*B*). Sensor activation was recovered by treatment of the inhibited cells with a chemical NO donor, SNAP (Fig. 3*B*). We next tested the *S*-nitrosylation hypothesis using a mutant form of the FRET-GCK probe (V367M) that prevents GCK nitrosylation without affecting GCK activity (17). GLP-1 treatment did not activate the V367M-containing FRET-GCK probe. These results are consistent with GLP-1 stimulated post-translational activation of GCK through *S*-nitrosylation.

Role of GCK S-Nitrosylation in GLP-1 Potentiation of Glucose Metabolism—To quantify the extent that GCK *S*-nitrosylation contributes to the insulinotropic effects of GLP-1, we first examined the effect of GCK(V367M) expression on glucose metabolism. Expression of GCK(V367M)-mCherry did not significantly affect the glucose-stimulated increase in NAD(P)H fluorescence compared with cells expressing WT GCK-mCherry (Fig. 4*A*); however, the effect of GLP-1 was completely diminished in cells expressing GCK(V367M)-mCherry. In islets, L-NAME inhibited GLP-1 potentiation of glucose metabolism but did not affect the rise in NAD(P)H autofluorescence observed with only glucose (Fig. 4*B*). GLP-1 did not affect NAD(P)H fluorescence in the absence of glucose.

Role of GCK S-Nitrosylation in GLP-1 Potentiation of Granule Exocytosis—We explored the role of GCK *S*-nitrosylation on GLP-1 potentiation of insulin secretion by using a TIRFM-based assay to quantify secretory granule fusion in individual βTC3 cells expressing a pH-sensitive fluorescent protein targeted to the lumen of the secretory granule. For these experiments, we used superecliptic pHluorin (SEP) fused to the C terminus of vesicle-associated membrane protein 2 (VAMP2) (22). Alkalization of the vesicle lumen occurs when the fusion pore opens and the lumen interior equilibrates with the extracellular medium, producing a burst of fluorescence from the pH-sensitive fluorescent protein cargo. Use of TIRFM restricts illumination to the plasma membrane adjacent to the coverslip (23) and enables quantitative imaging of granule exocytosis (24–26). βTC3 cells were co-transfected with SEP-VAMP2 and either GCK-mCherry (Fig. 5*A*) or GCK(V367M)-mCherry (Fig. 5*B*) and imaged using TIRFM. A typical granule fusion event from a glucose-stimulated cell is shown in Fig. 5*C*. Bandpass filters were used to exclude the red mCherry fluorescence from the green SEP fluorescence during TIRFM, and no cross-talk fluorescence was observed. Furthermore, treatment with a calcium channel blocker prevented glucose-stimulated increases in SEP-VAMP2 fluorescence (supplemental Fig. S2), indicating that the quantified changes in SEP-VAMP2 fluorescence are consistent with granule exocytosis.

Glucose-starved cells were treated with 8 mM glucose to stimulate secretion (Fig. 5*D*). In cells expressing WT GCK-mCherry, glucose stimulation produced a modest increase in vesicle fusions. Addition of GLP-1 potentiated granule exocytosis in cells expressing both the WT and GCK(V367M)-mCherry proteins (Fig. 5, *D–F*). GLP-1 potentiation occurred largely during the first ~20 s following stimulation. Interestingly, the effect of GLP-1 on granule exocytosis during this time

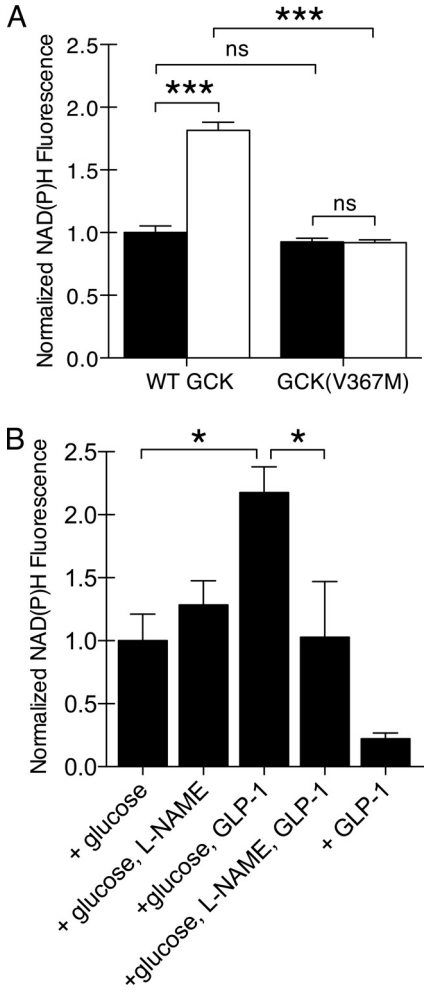

FIGURE 4. **Dependence of GLP-1-potentiated glucose metabolism on GCK *S*-nitrosylation.** *A*, changes in NAD(P)H fluorescence were observed by two-photon fluorescence microscopy for βTC3 cells expressing GCK-mCherry or GCK(V367M). Cells were stimulated with 5 mM glucose alone (*black*) or in combination with 30 nM GLP-1 (*white*). The NAD(P)H fluorescence at 3 min was normalized to basal, prestimulation fluorescence. *Bars* indicate mean ± S.E. (*error bars*), and statistical significance (ANOVA, $n = 5$, Tukey multiple comparison test) is indicated by symbols as follows: ***, $p < 0.001$; *ns*, $p > 0.05$. *B*, changes in islet NAD(P)H fluorescence were observed by two-photon microscopy. Islets were incubated with 2 mM glucose for 60 min prior to stimulation with 5 mM glucose and/or 30 nM GLP-1 as indicated. Prior to stimulation, some islets were pretreated with 5 mM L-NAME to inhibit NOS activity. *Bars* indicate mean ± S.E., and statistical significance (ANOVA, $n = 5$, Tukey multiple comparison test) is indicated by * ($p < 0.05$).

frame was similar in magnitude to insulin secretion from untransfected βTC3 cells measured by ELISA (Fig. 5*G*). Expression of GCK(V367M)-mCherry did not significantly affect glucose responsiveness (Fig. 5, *E* and *F*), but reduced the effect of GLP-1 by ~40%. These results suggest that regulation of GCK activity is an important mechanism through which GLP-1 potentiates glucose-stimulated insulin secretion from pancreatic β cells.

DISCUSSION

Here, we have shown the effects of GLP-1 on β cell glucose metabolism that are linked with GCK activation by post-translational *S*-nitrosylation. Furthermore, regulation of glucose metabolism accounts for a substantial portion of the insulinotropic response in our model system. These findings may provide a mechanism through which GLP-1 reduces the glucose threshold for insulin secretion. Secretion is triggered by calcium ion influx through voltage-gated channels responding to an action potential. Closure of ATP-sensitive potassium channels is the primary mechanism controlling metabolism-triggered depolarization, and GLP-1 is known to modulate the function of these channels through a variety of mechanisms. For example, phosphorylation of the sulfonylurea receptor subunit has been shown to increase sensitivity to ADP in recombinant channels (27), and cAMP guanine nucleotide exchange factors can enhance sensitivity to the ATP modulatory component (28). Nonetheless, both of these mechanisms require a sufficient amount of glucose metabolism to change the ATP/ADP ratio, a process that is strongly limited by GCK activity.

The effect of GCK on secretory threshold is strongly supported by data using hexokinase overexpression (8, 9) systems and studies on naturally occurring GCK mutations that cause disease (6, 11). Mutations that increase GCK activity lower the secretory threshold, and conversely mutations that reduce GCK activity raise it. In the absence of mutations or exogenous expression to raise activity, half-maximal GCK activity occurs at ~8 mM glucose (4). Studies on ATP-sensitive potassium channel function found modulation of secretion with glucose concentrations as low as 5 mM (27), which is right at the threshold for glucose-stimulated insulin secretion (10). In the presence of GLP-1, however, insulin secretion has been observed at glucose concentrations as low as 3 mM (1). Using mathematical parameters to calculate the expected GCK activity for a given glucose concentration (4), glucose phosphorylation is calculated to be approximately two-thirds less at 3 mM than at 5 mM. The low activity of GCK at these glucose concentrations calls into question whether the described effects on potassium channel function can sufficiently explain the insulinotropic effects of GLP-1 at normally subthreshold glucose concentrations.

The ability of GLP-1 to regulate glucose metabolism positively has been a point of interest because β cell metabolism is known to control insulin secretion tightly. Enhancement of ATP production has been observed in GLP-1-treated MIN6 cells (29), but less compelling effects have been observed on islet metabolism using biochemical approaches (30). The difference in experimental observations may be related to differences in methodology, because the biochemical measures utilized long incubation periods of generally 30 min or greater where the effects of GLP-1 may be lost due to signal termination. GLP-1 receptors are internalized with a half-time less than 3 min (31), and receptor desensitization occurs within 15 min (32). Signaling through GLP-1 receptors has also been shown to peak within 15 min (33). In general, techniques with exceptional time resolution, such as NAD(P)H fluorescence used in this study or the luciferase technique employed by Tsuboi *et al.* (29), have been more successful at demonstrating regulation of metabolism by GLP-1. The mechanism proposed here is consistent with acute metabolic action that may be more difficult to detect over periods of 30–90 min. Highly focused work that looks specifically at GCK *S*-nitrosylation will undoubtedly be required to understand completely the effects of GLP-1 on islet metabolism.

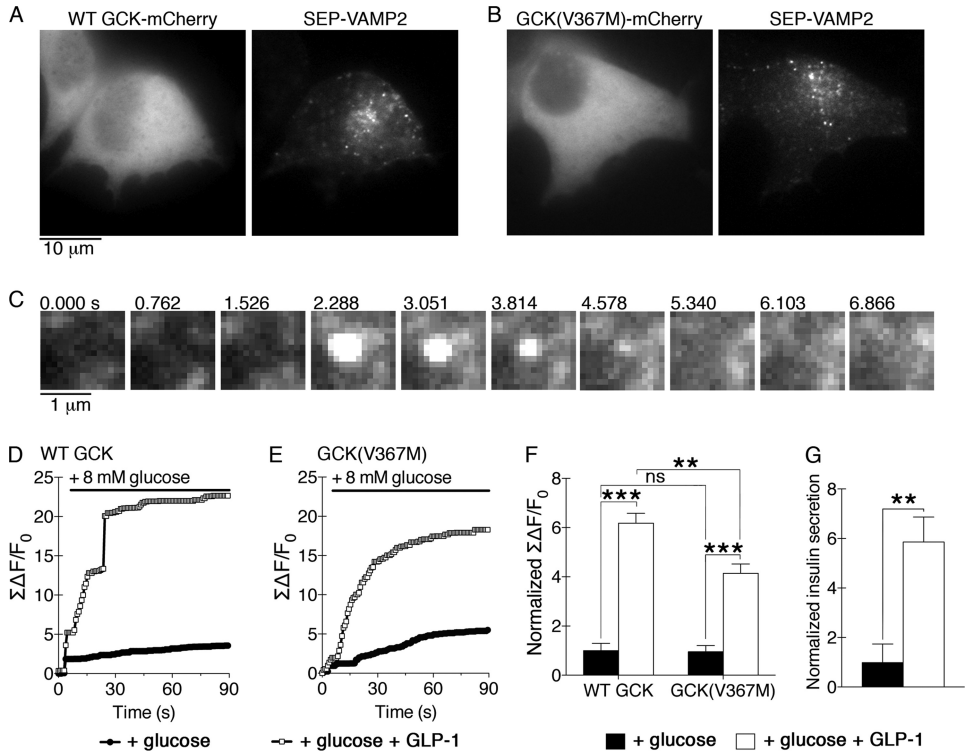

FIGURE 5. **GCK(V367M) expression diminishes GLP-1 potentiation of secretory granule fusion.** *A* and *B*, TIRFM was used to observe secretory granule fusion in βTC3 cells co-transfected with SEP-VAMP2 and either WT GCK-mCherry (*A*) or GCK(V367M)-mCherry (*B*). Red mCherry fluorescence was collected using widefield epifluorescence illumination, and SEP-VAMP2 fluorescence at the cell membrane adjacent to the coverslip was collected using TIRFM. *C*, membrane fusion of a SEP-VAMP2-labeled secretory granule during a typical exocytotic event is shown. *D*, sum change in membrane fluorescence over time is shown for SEP-VAMP2 fluorescence in βTC3 cells co-expressing WT-GCK-mCherry captured using TIRFM. Plots show a representative trace of a cell treated with either glucose alone (*black circles*) or pretreated with GLP-1 (30 nM, 10 min, *white squares*). *E*, representative traces as in *D* from cells co-expressing GCK(V367M)-mCherry are shown. *F*, sum changes in fluorescence were normalized to glucose-treated groups for 30 frames (22 s) following glucose stimulation for WT and V367M GCK-mCherry-expressing cells. *Bars* indicate mean ± S.E. (*error bars*), and statistical significance (ANOVA, $n = 5$, Tukey multiple comparison test) is indicated by symbols as follows: **, $p < 0.01$; ***, $p < 0.001$; *ns*, $p > 0.05$. *G*, insulin secretion from untransfected βTC3 cells was measured by ELISA. Cells were treated with glucose in the presence or absence of GLP-1 and normalized to results from glucose-treated cells. *Error bars* indicate S.E., and statistical significance was determined by *t* test (**, $p < 0.01$, $n = 5$).

We observed that the effects of GLP-1 on metabolism and GCK *S*-nitrosylation account for a substantial portion of the insulinotropic effect. GLP-1 treatment increased GCK activity by ~30% using the standard GCK activity assay which measures maximum velocity of GCK enzymatic activity at 100 mM glucose. This assay is largely insensitive to changes in glucose binding or other kinetic parameters, and the functional change in glucose metabolism we observe is a larger 2-fold increase in NAD(P)H fluorescence. This increase, and the ~40% decrease in secretion observed in GCK(V367M)-expressing cells, is likely to be fully explained by effects on GCK *S*-nitrosylation. We draw this conclusion because expression of GCK(V367M) completely reversed the effects of GLP-1 on GCK activation and glucose metabolism. Furthermore, expression of GCK(V367M) did not affect the metabolic or secretory response to glucose alone, indicating that expression of this mutant does not cause a general defect in glucose metabolism. Inhibition of GCK *S*-nitrosylation by expression of mutant proteins targets GCK *S*-nitrosylation more specifically than pharmacological manipulation of NOS signaling. We demonstrated that pharmacological inhibition of NOS can inhibit GCK activation, and addition of NO chemical can restore signaling. However, using pharmacological manipulation of NOS signaling to probe the effects of GCK *S*-nitrosylation on secretion is more problematic because there are many targets for NOS-mediated *S*-nitrosylation. Consequently, both positive (34, 35) and negative (36–38) regulation of secretion by NOS has been shown. Thus, NOS regulation of β cell function is fairly complex, and our studies suggest that NOS can be utilized in signaling systems that positively regulate secretion.

It is likewise intriguing to extrapolate our findings to the clinical phenotype of GCK(V367M) (39). Clearly, a defect in the ability of GLP-1 hormones to potentiate insulin secretion is consistent with the development of diabetes. On the other hand, the relationship between acute effects and chronic defects may be more complex. Davis *et al.* noted that recombinant GCK(V367M) is less stable than the WT GCK at temperatures in excess of 37 °C (6), suggesting a decrease in overall stability. In our transient transfection system we do find that GCK(V367M) is expressed in levels similar to those of the WT GCK protein (17), as opposed to the C220S mutant, which has severe temperature stability deficits (40) and decreased expression (17). Nonetheless, it is possible that a small decrease in GCK stability could have an additional impact on β cell function when chronically expressed given the extent that GCK controls insulin secretion. The relative importance of acute and chronic defects in explaining the clinical phenotype of GCK(V367M) will therefore require additional investigation.

Our initial estimate that GCK *S*-nitrosylation accounts for ~40% of the secretory response has some limitations given the lack of gap junctional connectivity in our βTC3 cells that strongly enhances secretory output (41). Further, the experiments were also not designed to take into account the oscillatory nature of secretion from a natural islet, nor the potential for metabolic oscillations (42). Nonetheless, activation of GCK could synergize with other GLP-1-dependent mechanisms such as regulation of ATP-sensitive potassium channels. Enhanced metabolic output combined with increased sensitivity of these channels to changes in the ADP/ATP ratio could work together and enhance the secretory response to glucose. Combining these effects with regulation of secretory granule dynamics (43, 44) would form a robust acceleration of insulin secretion with multiple regulatory mechanisms acting in concert.

In conclusion, we have shown GCK *S*-nitrosylation contributes to positive regulation of glucose metabolism by GLP-1. This mechanism provides an efficient mechanism through which GLP-1 lowers the secretory threshold and retains glucose dependence. Furthermore, this mechanism has the potential to synergize positively with other known mechanisms.

Acknowledgements—We thank Abisoluwa Adeyeye for assistance with biochemical measurement of GCK activity and Li-Ping He for assistance with pancreatic islet isolation.

REFERENCES

1. D'Alessio, D. A., Fujimoto, W. Y., and Ensinck, J. W. (1989) *Diabetes* **38,** 1534–1538
2. Weir, G. C., Mojsov, S., Hendrick, G. K., and Habener, J. F. (1989) *Diabetes* **38,** 338–342
3. Göke, R., Wagner, B., Fehmann, H. C., and Göke, B. (1993) *Res. Exp. Med.* **193,** 97–103
4. Matschinsky, F. M., Glaser, B., and Magnuson, M. A. (1998) *Diabetes* **47,** 307–315
5. Meglasson, M. D., Burch, P. T., Berner, D. K., Najafi, H., Vogin, A. P., and Matschinsky, F. M. (1983) *Proc. Natl. Acad. Sci. U.S.A.* **80,** 85–89
6. Davis, E. A., Cuesta-Muñoz, A., Raoul, M., Buettger, C., Sweet, I., Moates, M., Magnuson, M. A., and Matschinsky, F. M. (1999) *Diabetologia* **42,** 1175–1186
7. Matschinsky, F. M. (2002) *Diabetes* **51,** S394–404
8. German, M. S. (1993) *Proc. Natl. Acad. Sci. U.S.A.* **90,** 1781–1785
9. Wang, H., and Iynedjian, P. B. (1997) *Proc. Natl. Acad. Sci. U.S.A.* **94,** 4372–4377
10. Gloyn, A. L., Odili, S., Buettger, C., Njolstad, P. R., Shiota, C., Magnuson, M. A., and Matschinsky, F. M. (2004) in *Glucokinase and Glycemic Disease: From Basics to Novel Therapeutics* (Matschinsky, F. M., and Magnuson, M. A., eds) pp. 92–109, Karger, Basel
11. Gloyn, A. L., Noordam, K., Willemsen, M. A., Ellard, S., Lam, W. W., Campbell, I. W., Midgley, P., Shiota, C., Buettger, C., Magnuson, M. A., Matschinsky, F. M., and Hattersley, A. T. (2003) *Diabetes* **52,** 2433–2440
12. Stubbs, M., Aiston, S., and Agius, L. (2000) *Diabetes* **49,** 2048–2055
13. Arden, C., Trainer, A., de la Iglesia, N., Scougall, K. T., Gloyn, A. L., Lange, A. J., Shaw, J. A., Matschinsky, F. M., and Agius, L. (2007) *Diabetes* **56,** 1773–1782
14. Rizzo, M. A., and Piston, D. W. (2003) *J. Cell Biol.* **161,** 243–248
15. Hao, M., Head, W. S., Gunawardana, S. C., Hasty, A. H., and Piston, D. W. (2007) *Diabetes* **56,** 2328–2338
16. Rizzo, M. A., Magnuson, M. A., Drain, P. F., and Piston, D. W. (2002) *J. Biol. Chem.* **277,** 34168–34175
17. Ding, S. Y., Tribble, N. D., Kraft, C. A., Markwardt, M., Gloyn, A. L., and Rizzo, M. A. (2010) *Mol. Endocrinol.* **24,** 171–177
18. Patterson, G. H., Knobel, S. M., Arkhammar, P., Thastrup, O., and Piston, D. W. (2000) *Proc. Natl. Acad. Sci. U.S.A.* **97,** 5203–5207
19. Jaffrey, S. R., Erdjument-Bromage, H., Ferris, C. D., Tempst, P., and Snyder, S. H. (2001) *Nat. Cell Biol.* **3,** 193–197
20. Bennett, B. D., Jetton, T. L., Ying, G., Magnuson, M. A., and Piston, D. W. (1996) *J. Biol. Chem.* **271,** 3647–3651
21. Mayevsky, A., and Rogatsky, G. G. (2007) *Am. J. Physiol. Cell Physiol.* **292,** C615–640
22. Miesenböck, G., De Angelis, D. A., and Rothman, J. E. (1998) *Nature* **394,** 192–195
23. Axelrod, D. (1981) *J. Cell Biol.* **89,** 141–145
24. Michael, D. J., Geng, X., Cawley, N. X., Loh, Y. P., Rhodes, C. J., Drain, P., and Chow, R. H. (2004) *Biophys. J.* **87,** L03–05
25. Michael, D. J., Xiong, W., Geng, X., Drain, P., and Chow, R. H. (2007) *Diabetes* **56,** 1277–1288
26. Ohara-Imaizumi, M., Nishiwaki, C., Kikuta, T., Nagai, S., Nakamichi, Y., and Nagamatsu, S. (2004) *Biochem. J.* **381,** 13–18
27. Light, P. E., Manning Fox, J. E., Riedel, M. J., and Wheeler, M. B. (2002) *Mol. Endocrinol.* **16,** 2135–2144
28. Kang, G., Leech, C. A., Chepurny, O. G., Coetzee, W. A., and Holz, G. G. (2008) *J. Physiol.* **586,** 1307–1319
29. Tsuboi, T., da Silva Xavier, G., Holz, G. G., Jouaville, L. S., Thomas, A. P., and Rutter, G. A. (2003) *Biochem. J.* **369,** 287–299
30. Peyot, M. L., Gray, J. P., Lamontagne, J., Smith, P. J., Holz, G. G., Madiraju, S. R., Prentki, M., and Heart, E. (2009) *PLoS One* **4,** e6221
31. Widmann, C., Dolci, W., and Thorens, B. (1995) *Biochem. J.* **310,** 203–214
32. Widmann, C., Dolci, W., and Thorens, B. (1997) *Mol. Endocrinol.* **11,** 1094–1102
33. Vázquez, P., Roncero, I., Blázquez, E., and Alvarez, E. (2005) *J. Endocrinol.* **186,** 221–231
34. Smukler, S. R., Tang, L., Wheeler, M. B., and Salapatek, A. M. (2002) *Diabetes* **51,** 3450–3460
35. Kaneko, Y., Ishikawa, T., Amano, S., and Nakayama, K. (2003) *Am. J. Physiol. Cell Physiol* **284,** C1215–1222
36. Salehi, A., Carlberg, M., Henningson, R., and Lundquist, I. (1996) *Am. J. Physiol.* **270,** C1634–1641
37. Lajoix, A. D., Reggio, H., Chardès, T., Péraldi-Roux, S., Tribillac, F., Roye, M., Dietz, S., Broca, C., Manteghetti, M., Ribes, G., Wollheim, C. B., and Gross, R. (2001) *Diabetes* **50,** 1311–1323
38. Henningsson, R., Salehi, A., and Lundquist, I. (2002) *Am. J. Physiol. Cell Physiol.* **283,** C296–304
39. Velho, G., Blanché, H., Vaxillaire, M., Bellanné-Chantelot, C., Pardini, V. C., Timsit, J., Passa, P., Deschamps, I., Robert, J. J., Weber, I. T., Marotta, D., Pilkis, S. J., Lipkind, G. M., Bell, G. I., and Froguel, P. (1997) *Diabetologia* **40,** 217–224
40. Tiedge, M., Richter, T., and Lenzen, S. (2000) *Arch. Biochem. Biophys.* **375,** 251–260
41. Rocheleau, J. V., Remedi, M. S., Granada, B., Head, W. S., Koster, J. C., Nichols, C. G., and Piston, D. W. (2006) *PLoS Biol.* **4,** e26
42. Bertram, R., Sherman, A., and Satin, L. S. (2007) *Am. J. Physiol. Endocrinol. Metab.* **293,** E890–900
43. Kwan, E. P., and Gaisano, H. Y. (2005) *Diabetes* **54,** 2734–2743
44. Shibasaki, T., Takahashi, H., Miki, T., Sunaga, Y., Matsumura, K., Yamanaka, M., Zhang, C., Tamamoto, A., Satoh, T., Miyazaki, J., and Seino, S. (2007) *Proc. Natl. Acad. Sci. U.S.A.* **104,** 19333–19338